

Focusing inside negative index materials

Jeffrey B. Brock, Andrew A. Houck,^{a)} and Isaac L. Chuang^{b)}
Center for Bits and Atoms and Department of Physics, MIT, Cambridge, Massachusetts 02139

(Received 19 April 2004; accepted 28 July 2004)

Two key theoretical predictions for flat negative index lenses are that thicker lenses should have both internal and external foci, and that these foci should move linearly with small deviations in frequency. Two-dimensional electric field profiles of microwave transmission through rectangular slabs of composite wire and split-ring resonator material are presented. By scanning inside and outside the material, both internal and external foci are revealed. The power concentration around the internal focus is shown to have a negative curvature, consistent with the theoretical predictions. © 2004 American Institute of Physics. [DOI: 10.1063/1.1798398]

Until recently, a material with a negative index of refraction was only a theoretical curiosity.¹ However, the amazing potential of lenses made of these materials—a negative index lens could surpass the diffraction limit²—has excited a push towards developing new materials that exhibit this unique property. As a result, the experimental study of artificially constructed negative index media (NIM), sometimes called left-handed materials, has progressed rapidly in the past few years. The initial observation of negative refraction in composite wire and split ring resonator structures,^{3–5} once contested,^{6,7} has recently been confirmed by multiple groups.^{8,9} Research has since concentrated on the unique lensing properties of NIM, in contrast to positive index media (PIM), a flat homogeneous slab of NIM should act as a lens. Furthermore, a key theoretical prediction is that thicker slabs should also have an internal focus, with both the internal and external foci moving linearly as a function of frequency for small deviations. Currently, preliminary experimental evidence has been presented for flat slab lensing.^{9,10} However, no measurements of the internal behavior or dispersive properties of these materials has been presented.

Here, we present measurements of concentrations of power both inside and outside a rectangular slab of NIM, and measure the frequency response of these foci. In doing so, we see two previously unobserved features of focusing in wire-resonator NIM. By scanning inside the material, we observe a spatial map of the electric field with negative curvature; additionally, we find that the focal length increases with increasing frequency. In this paper, we first present simulations of ideal NIM and PIM used to predict these features of negative index focusing. We then present measurements of the two-dimensional (2D) electric field profile taken using a scannable 2D waveguide.

The electric field inside and outside of a flat slab of NIM focusing a point source should be shaped in a manner quantitatively different from that of a positive index slab. Figure 1 shows the results of ray-optic simulations of point source transmission through two ideal attenuating flat slabs: one with a negative index, one with a positive index. These simulations reveal two criteria for distinguishing negative index focusing and positive index transmission. First, a spatial concentration of power on the far side of the material is consis-

tent only with negative index focusing. For thicker slabs, the power maximum will be removed from the edge of the slab. The distance from the maximum to the edge of the slab, the focal length, is inversely proportional to the index of refraction in the small angle approximation; thus it should increase with the frequency of the incident radiation because the magnitude of the index decreases as a function of frequency.¹¹ Secondly, the curvature of the electric field profile will be different for positive and negative index materials, both inside the material and on the transmitted side. For a negative index material, we expect the contours in the electric field map to have negative curvature, whereas for a positive index material, we expect a broadened continuation of the positive curvature that one expects from a radial power law decay.

We test composite wire-resonator materials for these theoretically predicted focusing features. Previous experiments have demonstrated that these materials have a simultaneously negative electric permittivity and magnetic permeability, which combine to form a material that, when placed in a 2D waveguide, exhibits a negative index of refraction in a narrow bandwidth in the microwave regime.^{3,8,9} Previous materials were limited, however, in that they required the top plate of the waveguide to be lifted by several millimeters before they began to demonstrate negative index behavior. The split-ring and wire materials are designed to work with the top plate of the waveguide in contact with the material

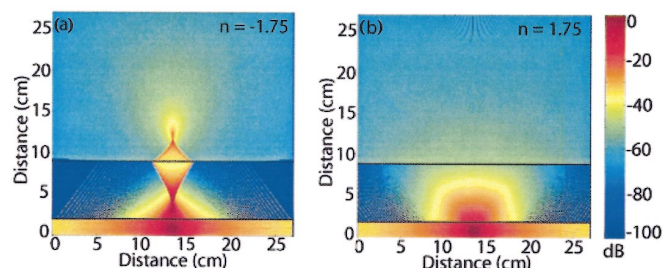


FIG. 1. (Color) Simulated transmission through NIM and PIM from a point source (at the bottom) through an ideal attenuating material (delineated by the solid black lines) 1 cm away, with depth 7 cm and width 27 cm. The plots are 2D distributions of power, represented by color, calculated by summing rays traced from the point source with appropriate phases. (a) The $n_r = -1.75$ simulation. There is a clear concentration of power on the far side of the slab that is not present in the positive index case. Furthermore, the field outside the slab of the negative index slab concentrates with a negative curvature that is absent in the positive index case. (b) The $n_r = 1.75$ simulation. There are no foci, only a broadened power law decay.

^{a)}Department of Physics, Harvard University, Cambridge, MA.

^{b)}Author to whom correspondence should be addressed; electronic mail: ichuang@mit.edu

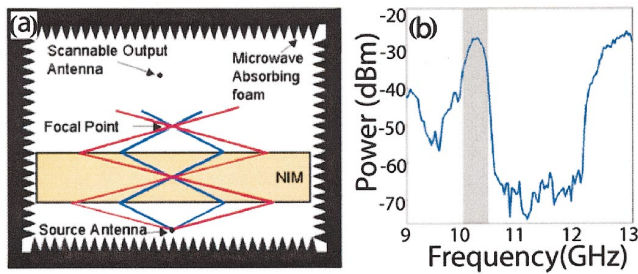


FIG. 2. (Color) Apparatus and material properties. (a) A schematic of the focusing setup. Flat slabs of negative index material were placed between the source antenna and the output antenna in the scannable waveguide. The 2D electric field profile was sampled both inside the material and in the transmitted region. (b) Transmission through composite material. The NIM passband (shaded gray) emerges from the region of low transmission (where either ϵ or μ are negative) as a narrow bandwidth centered at 10.3 GHz. The peak in transmission power of the passband is 35 dB higher than the low transmission floor.

with material parameters given in Ref. 11. The materials were constructed out of 50- μ m-thick copper on a 0.5 mm GML-1000 circuit board substrate (AP Circuits), with a 5 mm lattice constant. To improve the conductance of the circuit elements and decrease material attenuation, the circuit elements were coated with gold (Electroless Gold Solution, Transene Co).

Microwave point source transmission was measured through flat slabs of this material. A typical slab measured 40 cm wide and 7 cm deep. Measurements were taken using a 2D waveguide with scannable antenna.⁹ The input dipole antenna and materials are affixed to an aluminum plate that serves as the bottom of the 2D waveguide. The output dipole antenna is in the center of a parallel aluminum plate, twice as large in each dimension. The smaller plate is mounted on a 2D translation stage; as it moves, the only change in the configuration is the relative position of the output antenna. In this way, we can scan an output antenna throughout our waveguide. Additionally, our top plate can be raised and lowered via stepper motors; we can thus place our output antenna inside each of the cells of the NIM, measuring the field profile inside our composite material. The input power was sourced by an HP 8763E synthesized generator, and the output power was measured by an Agilent E4407B spectrum analyzer. In a typical measurement, a flat slab was placed at a distance of 1 cm from the source antenna, and the external data scans contained 40×120 data points [see Fig. 2(a)]. The resolution of scans taken inside of the material, however, was

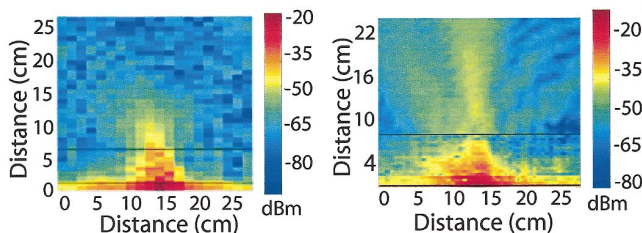


FIG. 3. (Color) Electric field inside and outside NIM slabs. Power measurements were taken of point source transmission through a 5 cm NIM slab (left) and a 7 cm NIM slab (right), whose boundaries are marked by solid black lines. Both slabs show negative curvature internally. The focal point for the 5 cm slab is at the edge of the material, while it is removed from the edge in the 7 cm slab.

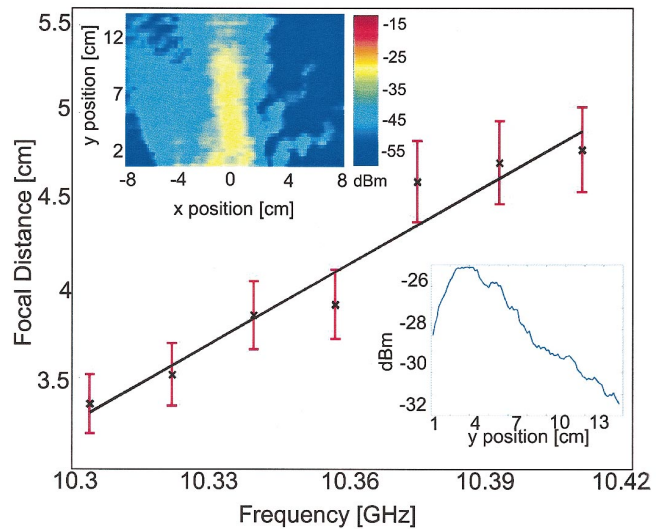


FIG. 4. (Color) Focal distance versus frequency. Point source transmission through a 7 cm NIM slab was observed as a function of frequency in the passband. Each data point is extracted from a 2D scan (top left inset) by taking several line scans vertically through the region of highest power (bottom right inset), and finding the peak power of these one-dimensional scans. Measured data are shown as points with error bars, with linear fit. Focal distance increases with frequency, as predicted.

limited by the dimensions of the antenna and the cell matrix to one data point per cell.

In order to find the frequency band in which our materials behave with a negative index, transmission measurements of point source radiation were taken over a wide frequency range. Transmitted power was sampled at several points and averaged. As seen in Fig. 2(b), a high transmission region in the transmitted power, centered at 10.3 GHz, was interpreted as the negative index regime.⁴ This is in agreement with the theoretically predicted properties of this material.¹¹

The two negative index focusing criteria were investigated with measurements of transmitted power from a 10.4 GHz point source through two NIM slabs, 5 and 7 cm deep. Typical scans can be seen in Figs. 3(a) and 3(b). Both slabs show highly aberrated concentrations of power, although in the 5 cm slab, the power is highest in the tip of a pyramidal shaped region at the edge of the slab. This is consistent with negative index focusing through shallow slabs; the nonaberrated “perfect focus” is only expected for lossless $n=-1$ slabs. The focal point of the 7 cm slab is separated from the slab, which is consistent with NIM focusing in deeper slabs. Power measurements in both slabs clearly show concentrations of power that are inconsistent with a positive index material. The contours internal to the slab have negative curvature in both slabs. There is no evidence of either broad collimation, or broadened power law decay, the signatures of a positive index attenuator. Thus it is concluded that evidence consistent with negative index focusing has been observed in both flat slabs.

We test that focal length increases with increasing frequency by making several transmission measurements through the 7 cm slab, varying the frequency of the source. The focal point of each measurement was determined by averaging several high-resolution single-line scans taken vertically through the region of highest transmitted power. As shown in Fig. 4, the focal distance was determined by fitting

a curve to the region of maximum power in their vertical scans, and finding the distance at which the peak power occurred. Between 10.3 and 10.42 GHz over a narrow bandwidth consistent with the NIM passband, the focal distance increased with frequency.

Collectively, this evidence demonstrates that we have observed behavior that is consistent with focusing from a composite wire-resonator structure. We have experimentally observed two previously unobserved criteria for discerning negative index focusing. First, we measured the field inside the NIM, and showed that the contours in the internal electric field profile have negative curvature. Additionally, we demonstrated a linear dependence of the focal length on the frequency. However, the promise of subwavelength resolution remains experimentally elusive in these wire-split-ring-resonator materials, although subwavelength resolution has been reported in other NIM.^{12,13} Further material improvements are needed before these theoretical predictions can be accurately tested.

This work is funded by the NSF Center for Bits and Atoms and MURI Award No. F49620-03-1-0420. One of the

authors (A. A. H.) gratefully acknowledges support from the Hertz Foundation.

¹V. G. Veselago, *Sov. Phys. Usp.* **10**, 509 (1968).

²J. B. Pendry, *Phys. Rev. Lett.* **85**, 3966 (2000).

³R. A. Shelby, D. R. Smith, and S. Schultz, *Science* **292**, 77 (2001).

⁴R. A. Shelby, D. R. Smith, S. C. Nemat-Nasser, and S. Schultz, *Appl. Phys. Lett.* **78**, 489 (2000).

⁵D. R. Smith, S. Schultz, P. Markos, and C. M. Soukoulis, *Phys. Rev. B* **65**, 195103 (2002).

⁶P. M. Valanju, R. M. Walser, and A. P. Valanju, *Phys. Rev. Lett.* **88**, 187401 (2002).

⁷N. Garcia and M. Nieto-Verperinas, *Phys. Rev. Lett.* **88**, 207403 (2002).

⁸C. G. Parazzoli, R. B. Greegor, K. Li, B. E. C. Koltenbah, and M. Tanielian, *Phys. Rev. Lett.* **90**, 107401 (2003).

⁹A. A. Houck, J. B. Brock, and I. L. Chuang, *Phys. Rev. Lett.* **90**, 137401 (2003).

¹⁰P. Parimi, W. T. Lu, P. Vodo, and S. Sridhar, *Nature (London)* **426**, 404 (2003).

¹¹C. D. Moss, T. M. Grzegorzczuk, Y. Zhang, and J. A. Kong, *Prog. Electromagn. Res.* **35**, 315 (2002).

¹²A. Grbic and G. V. Eleftheriades, *Phys. Rev. Lett.* **92**, 117403 (2004).

¹³N. Lagarkov and V. N. Kissel, *Phys. Rev. Lett.* **92**, 077401 (2004).